

# Quasi-Periodic Parallel WaveGAN Vocoder: A Non-autoregressive Pitch-dependent Dilated Convolution Model for Parametric Speech Generation

Yi-Chiao Wu<sup>1</sup>, Tomoki Hayashi<sup>1</sup>, Takuma Okamoto<sup>2</sup>, Hisashi Kawai<sup>2</sup>, and Tomoki Toda<sup>1,2</sup>

<sup>1</sup>Nagoya University, Japan

<sup>2</sup>National Institute of Information and Communications Technology, Japan

yichiao.wu@g.sp.m.is.nagoya-u.ac.jp, tomoki@icts.nagoya-u.ac.jp

## Abstract

In this paper, we propose a parallel WaveGAN (PWG)-like neural vocoder with a quasi-periodic (QP) architecture to improve the pitch controllability of PWG. PWG is a compact non-autoregressive (non-AR) speech generation model, whose generation speed is much faster than real-time. While PWG is taken as a vocoder to generate speech on the basis of acoustic features such as spectral and prosodic features, PWG-generated speech contains a high fidelity. However, because of the fixed and generic network structure, the pitch accuracy of PWG-generated speech degrades when the PWG vocoder conditioned on the acoustic features including unseen pitch features such as scaled pitches. The proposed QPPWG adopts a pitch-dependent dilated convolution network (PDCNN) module, which introduces the pitch information into PWG via the dynamically changed network architecture, to improve the pitch controllability and speech modeling capability of vanilla PWG. Both objective and subjective evaluation results confirm the higher pitch accuracy and comparable speech quality of QPPWG-generated speech, while the QPPWG model size is only 70 % of that of vanilla PWG.

**Index Terms:** neural vocoder, parallel WaveGAN, quasi-periodic WaveNet, pitch-dependent dilated convolution

## 1. Introduction

Because of the high temporal resolution of speech signals, speech waveform modeling is challenging. The general technique to tackle speech synthesis (SS) is called a vocoder [1, 2], which encodes waveforms into low-dimensional acoustic features and decodes waveforms on the basis of the acoustic features. The conventional vocoders such as STRAIGHT [3] and WORLD (WD) [4] are usually designed on the basis of a source-filter model [5], which decomposes speech into spectral and prosodic acoustic features. However, the hand-crafted signal-processing mechanisms of the conventional vocoders cause the loss of phase information and temporal details, which results in speech quality degradation.

To achieve high fidelity SS, many neural network (NN)-based autoregressive (AR) SS models, which directly model the probability distributions of speech waveforms without many hand-crafted assumptions of SS, such as WaveNet (WN) [6] and SampleRNN [7] have been proposed. The NN-based vocoders [8–13], which replace the synthesizers of the conventional vocoders to recover the lost phase information and temporal details, are also proposed on the basis of these AR SS models to generate high-quality speech. Furthermore, because of the extremely slow generation time of the AR models, many non-AR models such as flow-based [14–18] and generative adversarial network (GAN) [19]-based models [20, 21] have been

proposed for practical SS applications such as text-to-speech (TTS) and voice conversion (VC).

However, because of the data-driven nature and the lack of prior speech knowledge, it is hard for these NN-based SS models to deal with unseen data. For instance, if the pitches of the testing acoustic features are scaled or outside the range of the training data, the pitch accuracy and speech quality of the WN-generated speech samples markedly degrade. Since the pitch controllability is an essential feature for a vocoder, NN-based SS models with carefully designed periodic and aperiodic inputs [22–24] greatly improve the pitch modeling capability. Furthermore, in our previous work, we proposed a quasi-periodic WN vocoder (QPNet) [25, 26], which adopts pitch-dependent dilated convolution networks (PDCNNs) to dynamically change the network architecture according to the input pitches, to improve the pitch controllability and speech modeling ability of WN. The proposed QP structure cannot be realized by recurrent NN-based models [12, 13].

In this paper, we further explore the effectiveness of the quasi-periodic (QP) structure for parallel WaveGAN (PWG) [15], which is a compact non-AR model with simple acoustic features and Gaussian noise inputs. Specifically, PWG transforms a noise sequence sampled from a standard Gaussian distribution into speech samples with acoustic features as the auxiliary feature, and it is more flexible than the models required specific periodic and aperiodic inputs. The non-AR nature also makes the generation process of PWG much faster than that of QPNet. Therefore, we apply the QP structure to PWG to develop a fast and flexible QPPWG vocoder with higher pitch controllability and a more compact model size. Both objective and subjective evaluations are conducted, and the experimental results show the higher pitch accuracy, comparable speech quality, and smaller model size of the QPPWG vocoder than that of the PWG vocoder.

## 2. Parallel WaveGAN

As shown in Fig. 1, PWG is composed of a discriminator ( $D$ ), a generator ( $G$ ), and a multi-resolution short-time Fourier transform (STFT) loss module. The discriminator is trained to detect synthesized samples as fake speech and natural samples as real speech, and its training criterion is to minimize the loss of discriminator ( $L_D$ ), which is formulated as

$$L_D(G, D) = \mathbb{E}_{\mathbf{x} \in p_{\text{data}}} [(1 - D(\mathbf{x}))^2] + \mathbb{E}_{\mathbf{z} \in N(0, I)} [D(G(\mathbf{z}))^2], \quad (1)$$

where  $\mathbf{x}$  denotes the natural samples,  $p_{\text{data}}$  denotes the data distribution of the natural samples,  $N(0, I)$  denotes a Gaussian distribution with zero mean and standard deviation, and  $\mathbf{z}$  denotes the input noise drawn from the Gaussian distribution for

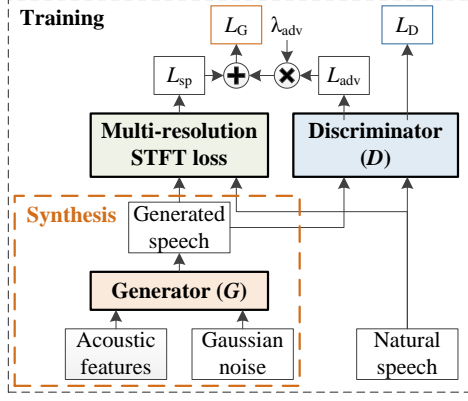


Figure 1: Architecture of Parallel WaveGAN.

the generator. Note that all auxiliary features of  $G$  are omitted in this chapter for simplicity. The discriminator is a fully-convolutional network (DCNN) [27] layers with LeakyReLU [28] activation functions. The dilation size of each DCNN layer is extending in an exponential growth manner with a base of two and an exponent of its layer index. The generator is trained to generate speech samples, which makes the discriminator difficult to distinguish between the synthesized and natural samples. The training criterion of the generator is to minimize the generator loss ( $L_G$ ) formulated as

$$L_G(G, D) = L_{sp}(G) + \lambda_{adv} L_{adv}(G, D), \quad (2)$$

which is the weighted sum of an adversarial loss ( $L_{adv}$ ) from the GAN structure and a spectral loss ( $L_{sp}$ ) from the multi-resolution STFT loss module with a weight  $\lambda_{adv}$ . The  $L_{adv}$  is formulated as

$$L_{adv}(G, D) = \mathbb{E}_{z \in N(0, I)} [(1 - D(G(z)))^2]. \quad (3)$$

Unlike flow-based models [14–18], which adopts an invertible network to transform the distribution of the input noise to the real data distribution, PWG adopts a GAN structure to make the generator learn the transformation via the feedback from the discriminator. The generator adopts a WN-like network but without the AR mechanism and causality, which make the generation time of PWG markedly faster than that of WN. To ensure the stability and efficiency of the GAN training, PWG adopts an extra  $L_{sp}$  as a regularizer of the generator. Specifically, the  $L_{sp}$  is composed of a spectral convergence loss ( $L_{sc}$ ) and a log STFT magnitude loss ( $L_{mag}$ ), which are formulated as

$$L_{sc}(\mathbf{x}, \hat{\mathbf{x}}) = \frac{\| |\text{STFT}(\mathbf{x})| - |\text{STFT}(\hat{\mathbf{x}})| \|_F}{\| |\text{STFT}(\mathbf{x})| \|_F}, \quad (4)$$

$$L_{mag}(\mathbf{x}, \hat{\mathbf{x}}) = \frac{1}{N} \|\log |\text{STFT}(\mathbf{x})| - \log |\text{STFT}(\hat{\mathbf{x}})|\|_{L1}, \quad (5)$$

where  $\hat{\mathbf{x}}$  denotes the generated samples from the generator,  $\|\cdot\|_F$  is Frobenius norm,  $\|\cdot\|_{L1}$  is  $L1$  norm,  $|\text{STFT}(\cdot)|$  denotes STFT magnitudes, and  $N$  is the number of the magnitude elements. Moreover, to avoid the generator overfitting to a specific STFT resolution causing a suboptimal problem, the final  $L_{sp}$  is a summation of several  $L_{sp}$  values calculated on the basis of STFT features with different analysis parameters such as FFT size and frame length and shift.

Although PWG achieves high fidelity speech generation, the fixed and generic network architecture of PWG is not appropriate. Specifically, since speech is a quasi-periodic signal

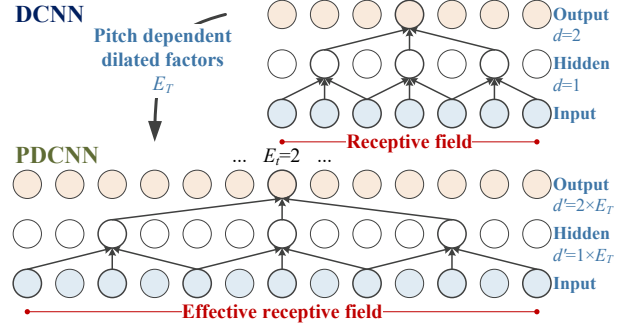


Figure 2: Pitch-dependent dilated convolution.

consisting of periodic and aperiodic components, which respectively have long-term and short-term correlations, the fixed architecture of PWG is not efficient for modeling speech. For instance, the same size of *receptive fields*, which are the regions in the input space that the outputs are affected by, for both periodic and aperiodic components is not optimized. The *receptive fields* may include many redundant samples for periodic parts. To tackle this problem, we proposed a QPPWG vocoder, which dynamically changes its architecture according to the input pitches, to improve the pitch controllability and speech modeling capability.

### 3. Quasi-Periodic parallel WaveGAN

Since the GAN architecture and the multi-resolution STFT loss of PWG have shown the effectiveness for training a speech generator, the proposed QPPWG focus on improving the generator using a QP structure while inherited the discriminator and the  $L_{sp}$  regularizer from PWG. The main modules of the QP structure are PDCNN components and a cascaded architecture, which are inspired by the pitch filtering and the cascaded recursive structure of the code-excited linear prediction (CELP) codec [29]. The details are as follows.

#### 3.1. Pitch-dependent dilated convolution

As shown in Fig. 2, there are gaps between the inputs of a DCNN kernel, and the length of each gap is a predefined hyperparameter called a dilation size (rate). PDCNN is an extension of DCNN, and its dilation size is pitch-dependent and dynamically changed according to the input pitch. Specifically, the dilated convolution is formulated as

$$\mathbf{y}_t^{(o)} = \mathbf{W}^{(c)} * \mathbf{y}_t^{(i)} + \mathbf{W}^{(p)} * \mathbf{y}_{t-d}^{(i)} + \mathbf{W}^{(f)} * \mathbf{y}_{t+d}^{(i)}, \quad (6)$$

where  $\mathbf{y}_t^{(i)}$  and  $\mathbf{y}_t^{(o)}$  are the input and output of the DCNN layer.  $\mathbf{W}^{(c)}$ ,  $\mathbf{W}^{(p)}$  and  $\mathbf{W}^{(f)}$  are the trainable  $1 \times 1$  convolution filters of current, previous, and following samples, respectively.  $*$  is the convolution operator, and the dilation size  $d$  of DCNN is a time-invariant constant. By contrast, PDCNN adopts a pitch-dependent dilated factor  $E_t$  to dynamically change the dilation size  $d'$  in each time step  $t$  as

$$d' = E_t \times d. \quad (7)$$

The dilated factor  $E_t$  is derived from

$$E_t = F_s / (F_0 \times t \times a), \quad (8)$$

where  $F_s$  is the sampling rate,  $F_0$  is the fundamental frequency, and  $a$  is a hyperparameter called a *dense factor*, which indicates the number of samples in one cycle taken as the PDCNN inputs

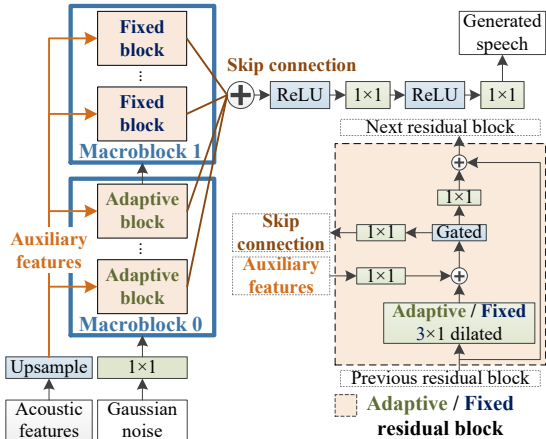


Figure 3: Architecture of QPPWG generator.

for each time step. The higher the *dense factor*, the lower the sparsity of PDCNN. In conclusion, QPPWG with the proposed PDCNN layers introduces the pitch information to the network, enables each sample to have a pitch-dependent length of its *receptive field*, and makes *receptive field* extending more efficient.

### 3.2. Generator of QPPWG

The architecture of the QPPWG generator is shown in Fig. 3, and it is similar to the WN-like PWG generator. The main difference is the hierarchical architecture of the stacked residual blocks. Specifically, QPPWG includes two cascaded macroblocks with different types of residual blocks while PWG only contains one type of residual blocks. The first macroblock of QPPWG consists of stacked adaptive blocks with PDCNN layers to model the periodic components with long-term correlations, and the second macroblock of QPPWG consists of stacked fixed blocks with DCNN layers to model the aperiodic components with short-term correlations.

## 4. Experiments

### 4.1. Model descriptions

In this paper, the QPPWG models with two different orders of macroblocks and the PWG models with two different numbers of residual blocks were evaluated. Specifically, the QPPWG model, whose first macroblock included 10 adaptive blocks with 2 cycles of the dilation size expansions ( $B_A10C2$ ) and the following macroblock included 10 fixed blocks with one cycle ( $B_F10C1$ ), was denoted as QPPWG<sub>af</sub> and the one with a reverse macroblock order was QPPWG<sub>fa</sub>. The generator of vanilla PWG (PWG<sub>30</sub>) contained 30 fixed blocks with 3 cycles ( $B_F30C3$ ) and the compact PWG (PWG<sub>20</sub>) contained 20 fixed blocks with 2 cycles ( $B_F20C2$ ). The channel and kernel sizes of the non-causal convolution of these generators were 64 and three. As shown in Table 1, the generator size of the proposed QPPWG is around 70 % of that of the vanilla PWG because of the less stacked residual blocks. However, because of the increased complexity of the network, the real time factor (RTF) of QPPWG generation with a Titan V GPU is around 0.018, which is higher than 0.016 of PWG<sub>30</sub> and 0.011 of PWG<sub>20</sub>. Moreover, the discriminators of these four models had the same architecture, which was 10 non-causal DCNN layers with 64 convolution channels, three kernels, and LeakyReLU ( $\alpha$  is 0.2) activation functions, and their sizes were around 0.1 M.

Table 1: Comparison of generator size ( $\times 10^6$ ).

	PWG		QPPWG	
	30	20	af	fa
Macro 0	$B_F30C3$	$B_F20C2$	$B_A10C2$	$B_F10C1$
Macro 1	-	-	$B_F10C1$	$B_A10C2$
Size	1.16	0.78	0.79	0.79

Table 2: Objective evaluation results.

	WD	PWG		QPPWG		
	-	30	20	af	fa	
		RMSE of $\log F_0$				
$1 \times F_0$	0.10	0.12	0.15	<b>0.11</b>	<b>0.11</b>	
$\frac{1}{2} \times F_0$	0.14	0.27	0.32	<b>0.19</b>	0.20	
$2 \times F_0$	0.10	0.15	0.15	<b>0.11</b>	<b>0.11</b>	
Average	0.11	0.18	0.21	<b>0.14</b>	<b>0.14</b>	
		MCD (dB)				
$1 \times F_0$	2.58	<b>3.69</b>	3.74	3.80	4.54	
$\frac{1}{2} \times F_0$	3.89	4.47	<b>4.39</b>	4.52	5.18	
$2 \times F_0$	3.79	5.24	5.06	<b>4.92</b>	5.61	
Average	3.42	4.46	<b>4.40</b>	4.41	5.11	

### 4.2. Experimental settings

All speech generation models were trained in a multi-speaker manner. The training corpus consisted of 2,200 utterances of the “slt” and “bdl” speakers of CMU-ARCTIC corpus [30] and 852 utterances of all speakers of Voice Conversion Challenge 2018 (VCC2018) corpus [31]. The total data length was around four hours. The testing corpus was the SPOKE set, which consisted of two male and two female speakers, of VCC2018 corpus, and the number of testing utterances of each speaker was 35. All speech data were set to a sampling rate of 22,050 Hz and a 16-bit resolution.

The auxiliary features of these speech generation models consisted of one-dimensional continuous  $F_0$ , one-dimensional unvoiced/voiced binary code ( $U/V$ ), 35-dimensional Mel-cepstrum (*mcep*), and two-dimensional coded aperiodicity (*codeap*). The WD vocoder was first adopted to extract one-dimensional  $F_0$  and 513-dimensional spectral feature (*sp*) and aperiodicity (*ap*) with a frameshift of 5 ms.  $F_0$  was interpolated to the continuous  $F_0$  and converted to the  $U/V$ , *ap* was coded into the *codeap*, and *sp* was parameterized into the *mcep*. To simulate unseen data, the continuous  $F_0$  was scaled by the ratios of 1/2 and 2 while keeping other features the same. Moreover, the dilated factor  $E_t$  of QPPWG was calculated with the continuous  $F_0$  because of the performance concern, and the *dense factor* of QPPWG was empirically set to four.

The models were trained with a RAdam optimizer [32] ( $\epsilon = 1e^{-6}$ ) with 400K iterations. For the stability, the generators of the models were trained with only multi-resolution STFT losses, which were calculated on the basis of three different FFT sizes (1024 / 2048 / 512), frameshifts (120 / 240 / 50), and frame lengths (600 / 1200 / 240), for the first 100K iterations and then jointly trained with the discriminators for the following 300K iterations. The balance weight  $\lambda_{adv}$  of  $L_{adv}$  was set to 4.0. The learning rates, which decayed 50 % every 200K iterations, of the generators were  $1e^{-4}$  and the discriminators were  $5e^{-5}$ . The minibatch size was six and the batch length was 25,520.

### 4.3. Objective evaluations

Root mean square error (RMSE) of  $\log F_0$  and Mel-cepstral distortion (MCD), which were calculated by the auxiliary features and the features extracted from the generated speech, were adopted to the objective evaluations. As shown in Table 2, the proposed QPPWG vocoders achieve markedly higher  $F_0$  accu-

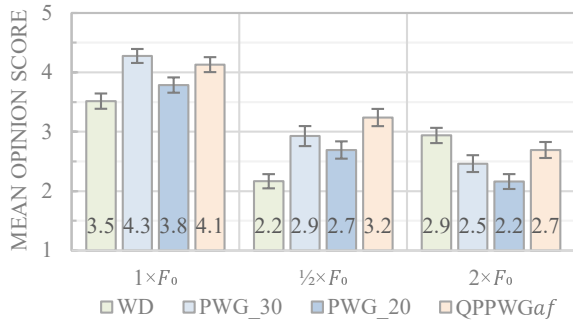


Figure 4: MOS results of speech quality with 95 % CI.

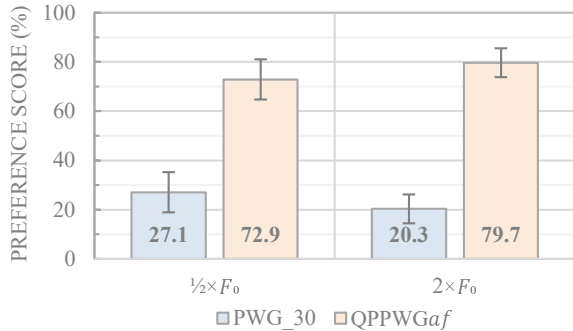


Figure 5: XAB results of pitch accuracy with 95 % CI.

racy than the PWG vocoders when conditioned on the scaled  $F_0$ , which confirms the effectiveness of the proposed QP structure. The results also show that QPPWG<sub>af</sub> achieves a comparable spectral prediction accuracy as the vanilla and compact PWGs. Moreover, QPPWG<sub>af</sub> outperforms QPPWG<sub>fa</sub> for the spectral accuracy, which implies that modeling long-term correlations first get a better overall spectral structure. In conclusion, the proposed QP structure improves the accuracy of pitch modeling of the PWG vocoder and efficiently extends the *receptive field* length, and the order of adaptive to fixed macroblocks is better than the reverse one.

#### 4.4. Subjective evaluations

The subjective evaluation set consisted of the 960 selected utterances of four testing speakers, four vocoders, which were WD, PWG\_30, PWG\_20, and QPPWG<sub>af</sub>, and three  $F_0$  scaled ratios, which were 1 (unchanged), 1/2, and 2. For each speaker, vocoder and  $F_0$  ratio, we randomly selected 20 utterances from the 35 testing utterances for both mean opinion score (MOS) and XAB tests. Specifically, the speech quality of each utterance was evaluated by listeners assigning MOSs (1–5). The higher the MOS, the better the speech quality. For the XAB test, every time listeners compared two testing utterances with one reference to pick up the utterance whose pitch contour was more consistent with that of the reference. The WD-generated utterances were taken as the references, and the pitch accuracies of the QPPWG<sub>af</sub>-generated utterances with 1/2 and 2  $F_0$  inputs were compared with that of the PWG\_30-generated ones. Eight listeners involved in both tests and each utterance was evaluated by at least two listeners.

As shown in Fig. 4, the QPPWG<sub>af</sub> vocoder markedly outperforms the same sized PWG\_20 vocoder for all  $F_0$  inputs. Even compared with PWG\_30, QPPWG<sub>af</sub> still achieves better speech qualities for the scaled  $F_0$  inputs and a comparable speech quality for the unchanged  $F_0$  input. In addition, the re-

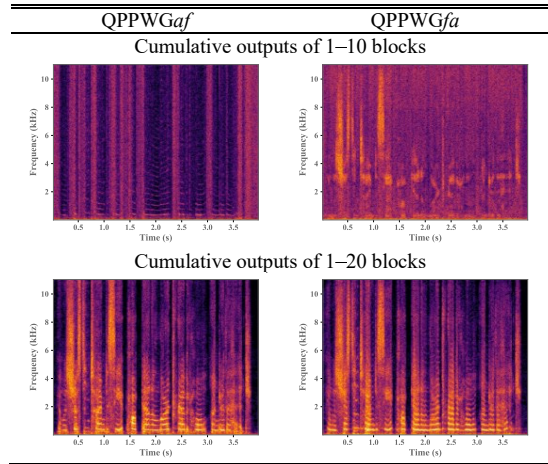


Figure 6: Comparison of intermediate cumulative.

sults of Fig. 5 show the perceptible differences of the pitch accuracies between the QPPWG<sub>af</sub> and PWG\_30 vocoders with scaled  $F_0$  inputs. In conclusion, introducing the pitch information to the PWG model by the QP structure markedly improves the pitch and speech modeling capabilities of the PWG vocoder, which results in compact model size and better pitch controllability of the QPPWG vocoder.

#### 4.5. Discussion

Since the model capacity is highly related to the *receptive field* length [25, 26], and the length of PWG\_30 is 6139 samples ( $2^0 + \dots + 2^9 = 1023$  with three cycles and two sides plus one), QPPWG attains an longer *effective receptive field* length around 3,000–16,000 samples. Specifically, the size is 2047 of the B<sub>F</sub>10C1 and  $124 \times E_T$  ( $2^0 + \dots + 2^4 = 31$  with two cycles and two sides) of the B<sub>A</sub>10C2, and the  $E_T$  is around 11–110 of the 500–50 Hz pitches when the *dense factor* is four.

Moreover, as the intermediate cumulative outputs shown in Fig. 6, the first ten adaptive blocks of QPPWG<sub>af</sub> focus on modeling the pitch and harmonic components, which have long-term correlations, while the first ten fixed blocks of QPPWG<sub>fa</sub> focus on modeling the non-harmonic components, which have short-term correlations. The results confirm our assumptions of the QP structure, and the behavior, which is similar to the harmonic plus noise model [33, 34], of QPPWG is more tractable and interpretable than that of vanilla PWG. More details and demo samples can be found on our website [35].

## 5. Conclusions

In this paper, we integrate a fast and compact PWG vocoder with a QP structure to improve its pitch controllability. The proposed QPPWG vocoder, whose model size is only 70 % of that of the PWG vocoder, achieves higher speech quality and pitch accuracy than the PWG vocoder when the input  $F_0$  sequence is scaled. In conclusion, the QPPWG vocoder is more in line with the definition of a vocoder.

## 6. Acknowledgments

This work was partly supported by JSPS KAKENHI Grant Number 17H06101 and JST, CREST Grant Number JP-MICR19A3 and PRESTO Grant Number JPMJPR1657.

## 7. References

- [1] H. Dudley, "The vocoder," *Bell Labs Record*, vol. 18, no. 4, pp. 122–126, 1939.
- [2] M. R. Schroeder, "Vocoders: Analysis and synthesis of speech," *Proc. IEEE*, vol. 54, no. 5, pp. 720–734, 1966.
- [3] H. Kawahara, I. Masuda-Katsuse, and A. de Cheveigné, "Restructuring speech representations using a pitch-adaptive time-frequency smoothing and an instantaneous-frequency-based F0 extraction: Possible role of a repetitive structure in sounds," *Speech Commun.*, vol. 27, no. 3–4, pp. 187–207, Apr. 1999.
- [4] M. Morise, F. Yokomori, and K. Ozawa, "WORLD: a vocoder-based high-quality speech synthesis system for real-time applications," *IEICE trans. Inf. Syst.*, vol. E99-D, no. 7, pp. 1877–1884, July 2016.
- [5] R. McAulay and T. Quatieri, "Speech analysis/synthesis based on a sinusoidal representation," *IEEE Trans Acoust. Speech Signal Process.*, vol. 34, no. 4, pp. 744–754, Aug. 1986.
- [6] A. van den Oord, S. Dieleman, H. Zen, K. Simonyan, O. Vinyals, A. Graves, N. Kalchbrenner, A. Senior, and K. Kavukcuoglu, "WaveNet: A generative model for raw audio," in *Proc. SSW9*, Sept. 2016, p. 125.
- [7] S. Mehri, K. Kumar, I. Gulrajani, R. Kumar, S. Jain, J. Sotelo, A. Courville, and Y. Bengio, "SampleRNN: An unconditional end-to-end neural audio generation model," in *Proc. ICLR*, Apr. 2017.
- [8] A. Tamamori, T. Hayashi, K. Kobayashi, K. Takeda, and T. Toda, "Speaker-dependent WaveNet vocoder," in *Proc. Interspeech*, Aug. 2017, pp. 1118–1122.
- [9] T. Hayashi, A. Tamamori, K. Kobayashi, K. Takeda, and T. Toda, "An investigation of multi-speaker training for WaveNet vocoder," in *Proc. ASRU*, Dec. 2017, pp. 712–718.
- [10] Z. Jin, A. Finkelstein, G. J. Mysore, and J. Lu, "FFNet: A real-time speaker-dependent neural vocoder," in *Proc. ICASSP*, Apr. 2018, pp. 2251–2255.
- [11] Y. Ai, H.-C. Wu, and Z.-H. Ling, "SampleRNN-based neural vocoder for statistical parametric speech synthesis," in *Proc. ICASSP*, Apr. 2018, pp. 5659–5663.
- [12] N. Kalchbrenner, E. Elsen, K. Simonyan, S. Noury, N. Casagrande, E. Lockhart, F. Stimberg, A. van den Oord, S. Dieleman, and K. Kavukcuoglu, "Efficient neural audio synthesis," in *Proc. ICML*, July 2018, pp. 2415–2424.
- [13] J.-M. Valin and J. Skoglund, "LPCNet: Improving neural speech synthesis through linear prediction," in *Proc. ICASSP*, May 2019, pp. 7830–7834.
- [14] A. van den Oord, Y. Li, I. Babuschkin, K. Simonyan, O. Vinyals, K. Kavukcuoglu, G. van den Driessche, E. Lockhart, L. C. Cobo, F. Stimberg, N. Casagrande, D. Grewe, S. Noury, S. Dieleman, E. Elsen, N. Kalchbrenner, H. Zen, A. Graves, H. King, T. Walters, D. Belov, and D. Hassabis, "Parallel WaveNet: Fast high-fidelity speech synthesis," in *Proc. ICML*, July 2018, pp. 3915–3923.
- [15] W. Ping, K. Peng, and J. Chen, "ClariNet: Parallel wave generation in end-to-end text-to-speech," in *Proc. ICLR*, May 2019.
- [16] R. Prenger, R. Valle, and B. Catanzaro, "WaveGlow: A flow-based generative network for speech synthesis," in *Proc. ICASSP*, May 2019, pp. 3617–3621.
- [17] S. Kim, S.-G. Lee, J. Song, J. Kim, and S. Yoon, "FloWaveNet: A generative flow for raw audio," in *Proc. ICML*, June 2019, pp. 3370–3378.
- [18] N.-Q. Wu and Z.-H. Ling, "WaveFFJORD: FFJORD-based vocoder for statistical parametric speech synthesis," in *Proc. ICASSP*, May 2020, pp. 7214–7218.
- [19] I. Goodfellow, J. Pouget-Abadie, M. Mirza, B. Xu, D. Warde-Farley, S. Ozair, A. Courville, and Y. Bengio, "Generative adversarial nets," in *Proc. NIPS*, Dec. 2014, pp. 2672–2680.
- [20] R. Yamamoto, E. Song, and J.-M. Kim, "Parallel WaveGAN: A fast waveform generation model based on generative adversarial networks with multi-resolution spectrogram," in *Proc. ICASSP*, May 2020, pp. 6199–6203.
- [21] K. Kumar, R. Kumar, T. de Boissiere, L. Gestin, W. Z. Teoh, J. Sotelo, A. de Brébisson, Y. Bengio, and A. C. Courville, "MelGAN: Generative adversarial networks for conditional waveform synthesis," in *Proc. NeurIPS*, Dec. 2019, pp. 14910–14921.
- [22] X. Wang, S. Takaki, and J. Yamagishi, "Neural source-filter-based waveform model for statistical parametric speech synthesis," in *Proc. ICASSP*, May 2019, pp. 5916–5920.
- [23] X. Wang, S. Takaki, and J. Yamagishi, "Neural source-filter waveform models for statistical parametric speech synthesis," *IEEE/ACM Transactions on Audio, Speech, and Language Processing*, vol. 28, pp. 402–415, 2020.
- [24] K. Oura, K. Nakamura, K. Hashimoto, Y. Nankaku, and K. Tokuda, "Deep neural network based real-time speech vocoder with periodic and aperiodic inputs," in *Proc. SSW10*, Sept. 2019, pp. 13–18.
- [25] Y.-C. Wu, T. Hayashi, P. L. Tobing, K. Kobayashi, and T. Toda, "Quasi-periodic WaveNet vocoder: A pitch dependent dilated convolution model for parametric speech generation," in *Proc. Interspeech*, Sept. 2019, pp. 196–200.
- [26] Y.-C. Wu, T. Hayashi, P. L. Tobing, K. Kobayashi, and T. Toda, "Quasi-periodic WaveNet: An autoregressive raw waveform generative model with pitch-dependent dilated convolution neural network," *IEEE/ACM Transactions on Audio, Speech, and Language Processing*, (submitted).
- [27] F. Yu and K. Vladlen, "Multi-scale context aggregation by dilated convolutions," in *Proc. ICLR*, May 2016.
- [28] A. L. Maas, A. Y. Hannun, and A. Y. Ng, "Rectifier nonlinearities improve neural network acoustic models," in *Proc. ICML*, June 2013, pp. 3–11.
- [29] M. Schroeder and B. Atal, "Code-excited linear prediction (CELP): High-quality speech at very low bit rates," in *Proc. ICASSP*, vol. 10, Apr. 1985, pp. 937–940.
- [30] J. Kominek and A. W. Black, "The CMU ARCTIC speech databases for speech synthesis research," in *Tech. Rep. CMU-LTI-03-177*, 2003.
- [31] J. Lorenzo-Trueba, J. Yamagishi, T. Toda, D. Saito, F. Villavicencio, T. Kinnunen, and Z. Ling, "The voice conversion challenge 2018: Promoting development of parallel and nonparallel methods," in *Proc. Odyssey*, June 2018, pp. 195–202.
- [32] L. Liu, H. Jiang, P. He, W. Chen, X. Liu, J. Gao, and J. Han, "On the variance of the adaptive learning rate and beyond," in *Proc. ICLR*, Apr. 2020.
- [33] Y. Stylianou, O. Cappé, and E. Moulines, "Continuous probabilistic transform for voice conversion," *IEEE Trans. Speech Audio Process.*, vol. 6, no. 2, pp. 131–142, 1998.
- [34] Y. Stylianou, "Applying the harmonic plus noise model in concatenative speech synthesis," *IEEE Trans. Speech Audio Process.*, vol. 9, no. 1, pp. 21–29, 2001.
- [35] Y.-C. Wu, "QPPWG demo," Accessed: 2020. [Online]. Available: [https://bigpon.github.io/QuasiPeriodicParallelWaveGAN\\_demo/](https://bigpon.github.io/QuasiPeriodicParallelWaveGAN_demo/).